

## FINAL REPORTS

### Vibrational and Electronic Properties of Fullerene and Carbon-Based Clusters

PI: Xiaoxing Xi

DOE Patent Clearance Granted

DE-FG02-84ER45095

*M P Dvorscak*

11-26-02

Mark P Dvorscak

Date

Reporting period: 7-1-1997 to 6-30-2001

(312) 252-2393

E-mail mark.dvorscak@ch.doe.gov

Office of Intellectual Property Law

DOE Chicago Operations Office

This project was under the direction of Prof. Xiaoxing Xi since September 1997 when the former PI, Prof. Jeff Lannin passed away. The main focus of the research has been in the lattice dynamics of ferroelectric thin films. In this report, we summarize the results of this project during this period and the publications resulted from this work.

## 1 Central importance of the soft mode in ferroelectrics

The potential of using ferroelectrics in various device applications have initiated a broad interest in the fundamental properties of ferroelectric thin films. For example, the ferroelectric properties are explored for non-volatile ferroelectric random-access memories (FRAM) [1, 2], the high static dielectric constant for dynamic random-access memories (DRAM) [3, 4] and gate oxide in MOSFET [5, 6], and the dielectric nonlinearity for tunable microwave devices [7].

Lattice dynamics is of central importance for ferroelectrics [8]. The hallmark of ferroelectricity, i. e. the spontaneous polarization, arises from a displacement of the center of positive charge with respect to the center of negative charge in the ferroelectric crystal. This displacement, such as that of the Ti ion with respect to the oxygen cage in the  $\text{TiO}_6$  octahedra in  $\text{BaTiO}_3$  (BTO), involves the same ionic movement as the vibration of a zone-center transverse optical phonon mode, the "soft mode". The soft mode has a low frequency due to the interplay between the local restoring force and the long range dipole interaction, and it decreases as the temperature is lowered. When the temperature approaches a Curie temperature  $T_c$ , the soft-mode frequency tends to zero [9, 10] and the soft mode is frozen in the crystal, which transforms to a ferroelectric phase [11]. The soft-mode theory, due to Cochran [11] and Anderson [12], has been proven by many lattice dynamics studies.

The soft-mode behavior can explain the high dielectric constant in the paraelectric phase of ferroelectrics. According to the Lyddane-Sachs-Teller (LST) relation, which connects the macroscopic dielectric constants to the microscopic parameter – optical phonon frequencies,

$$\frac{\epsilon(0)}{\epsilon(\infty)} = \prod_j^N \frac{\omega_{LOj}^2}{\omega_{TOj}^2}, \quad (1)$$

for a crystal with  $N$  optical modes. Here  $\epsilon(0)$  and  $\epsilon(\infty)$  are the static and the high frequency dielectric constants, and  $\omega_{LOj}$  and  $\omega_{TOj}$  are the frequencies of the longitudinal and transverse optical phonon modes, respectively. It is generally found that the frequencies of the higher optical modes exhibit no sizeable variation with temperature. The decrease in the soft-mode frequency as the temperature approaches  $T_c$  will thus cause a dramatic increase of  $\epsilon(0)$ . In bulk STO crystals

### DISCLAIMER

This report was prepared as an account of work sponsored by an agency of the United States Government. Neither the United States Government nor any agency thereof, nor any of their employees, makes any warranty, express or implied, or assumes any legal liability or responsibility for the accuracy, completeness, or usefulness of any information, apparatus, product, or process disclosed, or represents that its use would not infringe privately owned rights. Reference herein to any specific commercial product, process, or service by trade name, trademark, manufacturer, or otherwise does not necessarily constitute or imply its endorsement, recommendation, or favoring by the United States Government or any agency thereof. The views and opinions of authors expressed herein do not necessarily state or reflect those of the United States Government or any agency thereof.

## **DISCLAIMER**

**Portions of this document may be illegible in electronic image products. Images are produced from the best available original document.**

the LST relation has been proven experimentally:  $\epsilon(0)$  increases to values above 20000 as the temperature approaches a  $T_c$  of 32 K [9], although zero-point quantum fluctuations of Ti ions prevent a ferroelectric phase transition from occurring [13].

The soft-mode behavior is also the basis for the dielectric nonlinearity, i. e. the electric-field dependence of  $\epsilon(0)$ . It is due to the field-induced hardening of the soft mode frequency [14], which arises from the anharmonic restoring forces on the Ti ion when it is displaced from its equilibrium position [15]. According to the LST relation, a higher soft-mode frequency will lead to a decrease in the static dielectric constant. Another important materials parameter for applications is the dielectric loss. In an ideal ferroelectric crystal, it is related to the damping of the soft mode through multiple-phonon processes in the paraelectric phase, and dominated by the quasi-Debye contribution in the ferroelectric phase [15, 16, 17]. The study of lattice dynamical properties, in particular the soft-mode behavior, is essential for the fundamental understanding of the properties of ferroelectrics.

## 2 Symmetry breaking in STO films observed by Raman scattering

Lattice dynamical properties in bulk ferroelectrics, such as STO, BTO, etc., are well documented (see “Landolt-Börnstein numerical data and functional relationships in science and technology” [18, 19]). They can be studied using neutron scattering, Raman scattering, and infrared spectroscopy. However, there are few lattice dynamic studies in thin films, which is due to the difficulties in these measurements in transparent thin films. For example, in Raman scattering light goes through the film into the substrate, which has much larger scattering volume and therefore its signal dominates in the Raman spectrum. Same difficulties exist for infrared measurements as well.

To overcome the difficulties in measuring Raman scattering in transparent oxide thin films, we have used a metal-oxide bilayer Raman scattering (MOB-RS) technique, schematically shown in Fig. 1. A conducting metal oxide layer, such as of  $\text{YBa}_2\text{Cu}_3\text{O}_7$  (YBCO) or  $\text{SrRuO}_3$  (SRO), was deposited between the STO layer and the substrate. The conducting oxide layer reflects the substantial part of the laser beam back into the STO film and the rest attenuates quickly within the conducting layer, therefore Raman scattering from the substrate can be avoided and the signal from the STO film can be confidently detected. The thickness of this layer has to be thick enough, around 300 nm in our experiments, to block the signal from the substrate. In contrast to growing on substrates such as Pt/Si or  $\text{Al}_2\text{O}_3$ , the metal-oxide bilayer technique ensures high quality epitaxial growth of the ferroelectric thin films, which is important for probing intrinsic thin film properties.

In Fig. 2, Raman spectra of three STO films of different thicknesses in the STO/SRO/ $\text{LaAlO}_3$  (LAO) substrate bilayer structures measured at  $T = 5$  K are shown together with that of a single crystal. The Raman lines of the LAO substrate cannot be seen in the spectrum, indicating that the 300 nm SRO films are thick enough to effectively eliminate Raman signal from the substrate. Relatively weak features marked with stars are related to the SRO buffer layer [20]. The Raman scattering from the STO films is clearly observed. The use of MOB-RS technique is a critical step in our successful lattice dynamics studies of ferroelectric thin films. The report on the MOB-RS technique is published in Appl. Phys. Lett. [21].

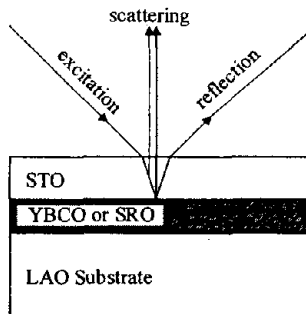


Figure 1: A schematic of metal-oxide bilayer Raman scattering. The conducting layer (YBCO or SRO) reflects the laser beam so that it cannot reach the substrate, allowing the study of Raman scattering from the STO thin film.

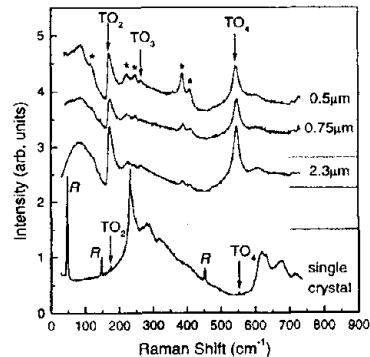


Figure 2: Normalized Raman spectra of STO films and a single crystal measured at  $T = 5$  K. The stars denote the SRO Raman lines,  $R$  the structural modes, and the arrows the zone center  $TO_{2,3,4}$  phonons.

Bulk STO crystals have a centrosymmetric structure: it is cubic at high temperatures and tetragonal below  $T_a = 105$  K. The zone-center optical phonons are of odd parity, and consequently are not Raman active [22]. The results of the STO thin films are very different, as shown in Fig. 2. By comparing with the hyper-Raman results of bulk single crystals [23, 24], where optical phonons are active, we identify the strong peak at  $170 \text{ cm}^{-1}$  as due to the  $TO_2$ , the weak peak at  $264 \text{ cm}^{-1}$  to the silent  $TO_3$ , and the strong peak at  $545 \text{ cm}^{-1}$  to the  $TO_4$  phonons. These peaks can be observed up to room temperature. In contrast, the Raman spectrum of the STO single crystal is characterized by the second-order scattering signal and the structural modes denoted by the letter  $R$ . Weak  $TO_2$  and  $TO_4$  peaks can also be seen in the single crystal spectrum, likely due to the impurities in the sample.

The appearance of the strong TO phonon peaks indicates a lowering of the crystal symmetry in the STO films, the breaking of inversion and/or translation symmetries. In Fig. 3, the enlarged spectra of the polar  $TO_{2,4}$  and non-polar  $TO_3$  peaks for the  $2.3 \mu\text{m}$  film are displayed for  $T = 5$  K. The  $TO_2$  peak is strongly asymmetric and exhibits a Fano profile [25]:

$$I(\omega) = A \frac{(q + E(\omega))^2}{1 + E(\omega)^2}, \quad (2)$$

where  $E(\omega) = 2(\omega - \omega_0)/\Gamma$ . Here  $\omega_0$  is the phonon frequency in the absence of interaction,  $\Gamma$  is its FWHM,  $A$  is the amplitude, and  $q$  is the asymmetry parameter. In contrast, the  $TO_3$  and  $TO_4$  peaks are mostly symmetric. The Fano effect occurs whenever discrete excitations and a broad continuum interfere coherently [25]. This continuum of excitations in STO films is polar because it only interacts with the polar  $TO_2$  phonon. In doped STO and KTO single crystals, the asymmetric line shape similar to that in Fig. 2(a) has also been found [26]. The polarization fluctuations in the defect-induced micro polar regions has been proposed to explain the asymmetry [27, 28]. The Fano effect in our STO films can similarly result from the interaction of the  $TO_2$  phonons with the polarization fluctuations in such local polar regions.

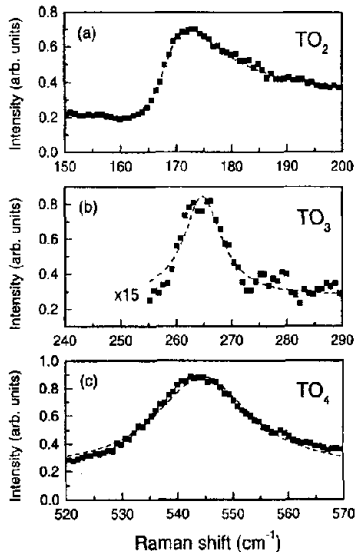


Figure 3: (a) The Fano-like TO<sub>2</sub> peak for a 2.3  $\mu\text{m}$  STO film at  $T = 5$  K. Dashed lines represent fits to the Fano profile. (b,c) The symmetric peaks for the TO<sub>3</sub> and TO<sub>4</sub> phonons, respectively.

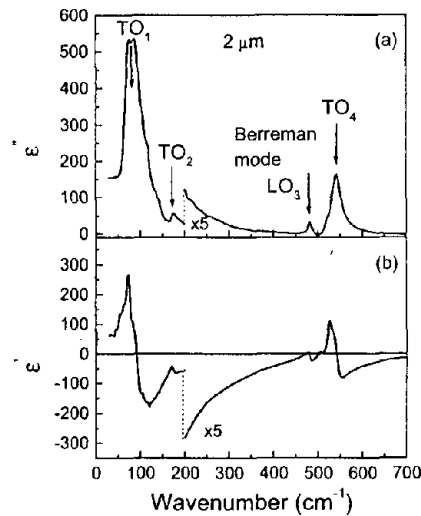


Figure 4: (a) The imaginary and (b) real parts of the effective dielectric function of a 2  $\mu\text{m}$ -thick STO film from far-infrared ellipsometry. Positions of the optical phonons are marked with arrows.

Concerning the origin of the local polar region, it is impossible to rule out the existence of impurities: even in samples of highest purity, acceptor-type impurities have been detected [29]. The defect chemistry studies show, however, that the existence of these impurities, as well as cation off-stoichiometry, often results in oxygen vacancies in the titanates [29]. It was shown by Uwe *et al.* that when a nominally pure STO single crystal is made oxygen deficient, ferroelectric micro-regions are induced in it [30]. Both theory and experiment show that the singly-charged oxygen vacancies give rise to dipole centers [31, 32]. In thin films, besides cation off-stoichiometry and acceptor-type impurities, oxygen vacancies can also result from insufficient oxygenation during the deposition process. Based on these considerations, we conclude that the local polar regions in the STO films are most likely caused by the oxygen vacancies.

The lattice dynamics evidence for defect related local polar regions has important implications for dielectric properties in ferroelectric thin film. The result is published in Phys. Rev. Lett. [33].

### 3 Soft-mode hardening in STO thin films

In the MOB-RS work described above, we did not detect the soft mode in the Raman spectra. For this purpose, we have performed far-infrared ellipsometry at the National Synchrotron Light Source (NSLS) at the Brookhaven National Laboratory. This newly developed technique combines ellipsometry, which directly measures the complex dielectric function without relying on the Kramers-Kronig transformation, with the Fourier-transform infrared (FTIR) spectroscopy, which allows a high throughput and multiplexing. Combined with the high brightness of the synchrotron radiation, it provides a powerful capability to measure vibrational properties with high reliability

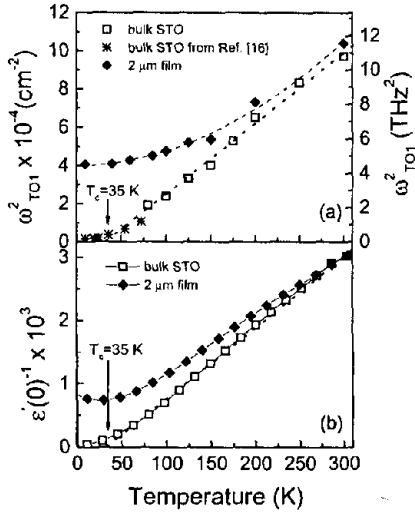


Figure 5: (a)  $\omega_{TO1}^2$  and (b)  $1/\epsilon(0)$  vs. temperature for a 2  $\mu\text{m}$ -thick STO film and an STO single crystal.

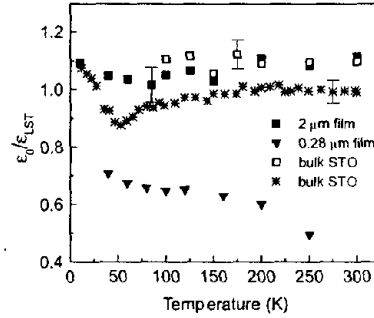


Figure 6: The data in Fig. 5 replotted as the ratio  $\epsilon(0)/\epsilon_{LST}$  versus temperature, where  $\epsilon(0)$  is the measured values and  $\epsilon_{LST}$  is the theoretical value based on the LST relation and calculated using the experimental values of the phonon frequencies. The result for a 0.28  $\mu\text{m}$ -thick STO film by Fedorov *et al* [36] is also included (triangles).

and accuracy. The real and imaginary parts of the effective dielectric function,  $\epsilon'(\omega)$  and  $\epsilon''(\omega)$ , from the far-infrared ellipsometry measurement of a 2  $\mu\text{m}$ -thick STO film at 200 K are shown in Fig. 4. The soft TO1 phonon mode is clearly observed along with other TO modes, and their positions are marked in the figure. The same general features were also observed in films of different thickness except that the spectral weight of the STO-SRO interface-related Berreman mode [34] decreases with increasing film thickness.

The soft-mode TO1 phonon frequency was measured as a function of temperature and the square of the soft-mode frequency,  $\omega_{TO1}^2$ , is plotted in Fig. 5 together with the inverse dielectric constant,  $1/\epsilon(0)$ , as obtained from the low-frequency dielectric measurements. Both the results for the STO film and a STO single crystal are displayed for comparison. As shown by Fig. 5(a), the frequency of the soft-mode decreases as the temperature is lowered. However, in clear contrast to the bulk crystals where the eigenfrequency of the TO1 phonon mode saturates at 13  $\text{cm}^{-1}$  at low temperature [35], in our STO thin film the TO1 eigenfrequency remains fairly high and saturates at 62  $\text{cm}^{-1}$ . Since the frequencies of the hard mode, the modes other than the soft mode, change only weakly with temperature and are completely the same as those in the bulk STO, a higher soft-mode frequency at low temperatures should lead to a lower the static dielectric constant  $\epsilon(0)$ , which is indeed observed as shown by Fig. 5(b). In Fig. 6, the ratio of the measured  $\epsilon(0)$  to the theoretical value  $\epsilon_{LST}$ , calculated according to Eq. (1) with the experimental phonon frequencies and the parameter  $\epsilon_\infty = 5.6$  [36], is plotted as a function of temperature. In the entire temperature range  $\epsilon(0)/\epsilon_{LST}$  remains almost constant and close to 1 for the STO crystal and the 1 and 2  $\mu\text{m}$  films. This demonstrates that, as in the bulk crystal, the LST relation between the measured optical phonon frequencies and the static dielectric constant is maintained with an accuracy of better than 10% in our 1 and 2- $\mu\text{m}$  STO thin films. In the thinner (0.28  $\mu\text{m}$ ) STO film by Fedorov *et al* [36], the LST relation was not fulfilled because the dead layer effect at the interface is more important for smaller film thickness.

The observation of the soft-mode hardening in STO films is important for such application of ferroelectrics as in DRAMs and MOSFET gate oxides. It has been found that the extremely high static dielectric constant  $\epsilon(0)$  in bulk ferroelectric materials tends to be significantly reduced in thin films [37]. This reduction in dielectric constant is often thought to arise at least to some extent from an interfacial “dead layer” which has a low dielectric constant [37, 38, 39]. Such a dead layer may arise from oxygen interdiffusion, chemical reaction, structural defects, Schottky barriers at the interfaces, or the electric-field penetration into the metal electrodes. Using a lattice dynamical approach to consider the interruption of dipole-dipole interaction by the interface, Zhou and Newns further pointed out that this dead layer effect is intrinsic [37]. Applying the dead layer model to STO films of various thicknesses we have derived a temperature-dependent dielectric constant for the volume of the film material which is only about 1000 at the maximum, i. e., still well below the value of  $\epsilon(0)$  in bulk single crystals [40]. Our infrared result shows that the low dielectric constant in STO thin films is due to the soft-mode hardening.

Our result provides direct experiment evidence linking the dielectric constant reduction to the fundamental lattice dynamics of ferroelectric thin films. The result is published in Nature [41].

#### 4 Electric-field induced soft-mode hardening in STO thin films

In STO single crystals, the dielectric nonlinearity, or the field tuning of  $\epsilon(0)$ , vanishes above  $T \sim 80$  K [42]. In thin films, on the other hand, the dielectric nonlinearity remains non-zero to very high temperature [43]. This property is important for applications of ferroelectric thin films in tunable microwave devices [7]. To find the mechanism of the dielectric nonlinearity in STO thin films, we have performed Raman scattering under external electric field.

The measured sample consisted of a  $0.2 \mu\text{m}$ -thick transparent conducting indium-doped tin oxide (ITO) top electrode deposited on a STO/SRO bilayer structure as in the MOB-RS [21]. The ITO top electrode allows the application of electric field normal to the film plane during the Raman measurements. The Raman response of the ITO layer is very weak compared to the STO film, and the Raman spectra from the coated and uncoated parts of the same STO film are essentially identical. Fig. 7(a) shows Raman spectra obtained at  $T = 5$  K with and without electric field. The external electric field applied normal to the film plane removes all centers of inversion in the crystalline structure of STO films making all optical phonons Raman active. The intensity change induced by the electric field is presented in Fig. 7(b). Strong maximum appears at about  $63 \text{ cm}^{-1}$  at  $T = 5$  K and its position shifts to higher frequencies when the temperature increases. The frequency and line shape of this maximum is similar to that of the soft mode  $\text{TO}_1$  phonon we have observed recently by far-infrared ellipsometry at zero field in the same sample [41]. Thus we attribute this Raman peak to the electric field-induced scattering by the soft mode phonon.

The temperature dependence of the  $\text{TO}_1$  phonon frequency,  $\omega_{\text{TO}_1}$ , for various external electric fields is shown in Fig. 8(a). The soft mode frequency increases when an electric field is applied, and the electric field induced soft-mode hardening is observed in the entire temperature range of the measurement. This is different from bulk crystals where the mode hardening vanishes above  $T \sim 80$  K [44]. Bulk STO crystals have a  $\text{TiO}_6$  cubic-to-tetragonal octahedral-rotation phase

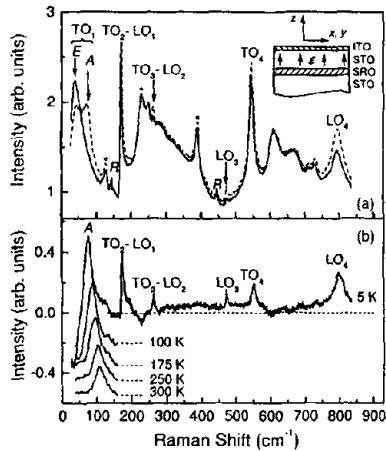


Figure 7: (a) Raman spectra of a  $1\ \mu\text{m}$  STO film with and without an external electric field of  $22 \times 10^4\ \text{V/cm}$ . (b) Electric-field-induced modification of the Raman intensity, i.e. the difference between spectra at  $\mathcal{E} = 22 \times 10^4\ \text{V/cm}$  and zero field, for different temperatures.

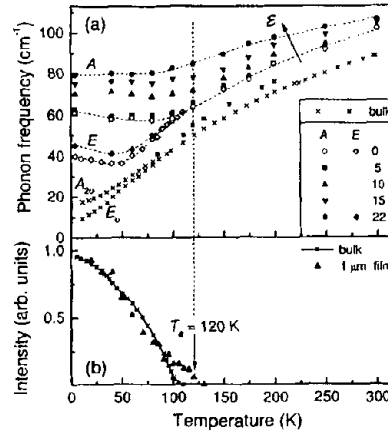


Figure 8: (a) Frequency of the  $\text{TO}_1$  phonon as a function of temperature for different values of external electric field, given in  $10^4\ \text{V/cm}$ . (b) Intensity of the structural  $R$  modes as a function of temperature. The structural cubic-to-tetragonal phase transition occurs in the film at about 120 K.

transition at 105 K [10]. As a result,  $R$ -point phonon modes become visible in the Raman spectrum below the phase transition temperature. The structural  $R$  modes are observed in our films at low temperature, and are marked by  $R$  in Fig. 7(a). In Fig. 8(b), the normalized  $R$ -mode intensity is shown as a function of temperature. The structural transition temperature in our films is found to be  $120 \pm 5\ \text{K}$ , higher than that in the bulk at 105 K. This observation is in a quantitative agreement with the x-ray diffraction result [45].

The electric-field dependence of  $1/\omega_{\text{TO}_1}^2$  is found to be consistent with that of  $\epsilon(0)$ , indicating the same mechanism for dielectric nonlinearity in films as in the bulk, i.e. the field induced hardening of the soft mode. The different dielectric nonlinearity in thin films is a reflection of the different soft-mode behavior from that in bulk crystals. The result is published in Phys. Rev. Lett. [46].

## 5 Publications resulting from the project

- 1 A. A. Sirenko, C. Bernhard, A. Golnik, A. M. Clark, Jianhua Hao, W. Si, and X. X. Xi, *Size effect and soft-mode hardening in  $\text{SrTiO}_3$  thin films*, Nature 404, 373 (2000).
- 2 I. A. Akimov, A. A. Sirenko, A. M. Clark, J.-H. Hao, and X. X. Xi, *Electric-field induced soft-mode hardening in  $\text{SrTiO}_3$  films*, Phys. Rev. Lett. 84, 4625 (2000).
- 3 J. R. Fox, I. A. Akimov, X. X. Xi, and A. A. Sirenko, *In situ Raman scattering studies of*

- amorphous and crystalline Si nanoparticles*, Solid State Communications 113, 553 (2000).
- 4 D. A. Tenne, A. M. Clark, A. R. James, K. Chen, and X. X. Xi, *Soft phonon modes in Ba<sub>0.5</sub>Sr<sub>0.5</sub>TiO<sub>3</sub> thin films studied by Raman spectroscopy*, Appl. Phys. Lett. 79, 3836 (2001).
  - 5 X. X. Xi, Anna M. Clark, J. H. Hao, and Weidong Si, *Dielectric and Lattice Dynamical Properties of SrTiO<sub>3</sub> Thin Films*, Integrated Ferroelectrics 28, 247 (2000).
  - 6 A. A. Sirenko, I. A. Akimov, J. R. Fox, A. M. Clark, H. -C. Li, W. Si, and X. X. Xi, *Observation of the first-order Raman scattering in SrTiO<sub>3</sub> thin films*, Phys. Rev. Lett. 82, 4500 (1999).
  - 7 X. X. Xi, H. -C. Li, W. Si, and A. A. Sirenko, *Dielectric properties and applications of strontium titanate thin films for tunable electronics*, in Nano-Crystalline and Thin Film Magnetic Oxides, eds. I. Nedkov and M. Ausloos, (Kluwer Academic Publishers, Dordrecht, 1999), p. 195.
  - 8 J. R. Fox, I. A. Akimov, X. X. Xi, and A. A. Sirenko, *In situ studies of the vibrational and electronic properties of Si nanoparticles*, MRS Symposium Proceeding 536, 287 (1999).
  - 9 V. I. Merkulov, J. R. Fox, H. -C. Li, W. Si, A. A. Sirenko, and X. X. Xi, *Metal-oxide bilayer Raman scattering in SrTiO<sub>3</sub> thin films*, Appl. Phys. Lett. 72, 3291 (1998).
  - 10 A. A. Sirenko, C. Bernhard, A. Golnik, I. A. Akimov, A. M. Clark, J.-H. Hao, and X. X. Xi, *Soft-mode phonons in SrTiO<sub>3</sub> thin films studied by far-infrared ellipsometry and Raman scattering*, MRS Symp. Proc. 603, 245 (2000).
  - 11 A. A. Sirenko, I. A. Akimov, C. Bernhard, A. M. Clark, J.-H. Hao, Weidong Si, and X. X. Xi, *Lattice dynamical properties of SrTiO<sub>3</sub> thin films*, to appear in AIP Proceedings.
  - 12 A. A. Sirenko, P. Etchegoin, A. Fainstein, K. Eberl, and M. Cardona, *Linear birefringence in GaAs/AlAs multiple quantum wells*, physica status solidi (b), 215, 241 (1999).
  - 13 A. A. Sirenko, P. Etchegoin, A. Fainstein, K. Eberl, and M. Cardona, *Birefringence in the transparent region of GaAs/AlAs multiple quantum wells*, Phys. Rev. B 60, 8253 (1999).

## References

- [1] J. F. Scott and C. A. Paz de Araujo, "Ferroelectric memories", *Science* 246, 1400 (1989).
- [2] O. Auciello, J. F. Scott, and R. Ramesh, "The physics of ferroelectric memories", *Physics Today* 51, 22 (1998).
- [3] A. I. Kingon, S. K. Streiffer, C. Basceri, and S. R. Summerfelt, "High-permittivity perovskite thin films for dynamic random-access memories", *MRS Bulletin* 21 No.7, 46 (1996).
- [4] D. E. Kotecki, J. D. Baniecki, H. Shen, R. B. Laibowitz, K. L. Saenger, J. J. Lian, T. M. Shaw, S. D. Athavale, C. Cabral, Jr., P. R. Duncombe, M. Gutsche, G. Kunkel, Y. J. Park, Y. Y. Wang, and R. Wise, "(Ba,Sr)TiO<sub>3</sub> dielectrics for future stacked-capacitor (DRAM)", *IBM J. Res. Develop.* 43, 367 (1999).
- [5] R. A. McKee, F. J. Walker, and M. F. Chisholm, "Crystalline oxides on silicon: The first five monolayers", *Phys. Rev. Lett.* 81, 3014 (1998).
- [6] K. Eisenbeiser, J. M. Finder, Z. Yu, J. Ramdani, J. A. Curless, J. A. Hallmark, R. Droopad, W. J. Ooms, L. Salem, S. Bradshaw, and C. D. Overgaard, "Field effect transistors with SrTiO<sub>3</sub> gate dielectric on Si", *Appl. Phys. Lett.* 76, 1324 (2000).
- [7] X. X. Xi, Hong-Cheng Li, Weidong Si, A. A. Sirenko, I. A. Akimov, J. R. Fox, A. M. Clark, and Jianhua Hao, "Oxide thin films for tunable microwave devices", *J. Electroceramics* 4, 407 (2000).
- [8] M. E. Lines and A. M. Glass, *Principles and applications of ferroelectrics and related materials* (Clarendon Press, Oxford) (1977).
- [9] J. L. Servoin, Y. Luspain, and F. Gervis, "Infrared dispersion in SrTiO<sub>3</sub> at high temperature", *Phys. Rev. B* 22, 5501 (1980).
- [10] G. Shirane and Y. Yamada, "Lattice-dynamical study of the 110 °K phase transition in SrTiO<sub>3</sub>", *Phys. Rev.* 177, 858 (1969).
- [11] W. Cochran, "Crystal stability and the theory of ferroelectricity", *Advan. Phys.* 9, 387 (1960).
- [12] P. W. Anderson, in "Fizika Dielektrikov", G. I. Skanavi, ed. (Akademika Nauk S.S.S.R. Fizicheskii Inst. im P. N. Lebedeva, Moscow) (1960).
- [13] K. A. Müller and H. Burkard, "SrTiO<sub>3</sub>:an intrinsic quantum paraelectric below 4 K", *Phys. Rev. B* 19, 3593 (1979).
- [14] J. M. Worlock and P. A. Fleury, "Electric field dependence of optical-phonon frequencies", *Phys. Rev. Lett.* 19, 1176 (1967).
- [15] G. Rupprecht, R. O. Bell, and B. D. Silverman, "Nonlinearity and microwave losses in cubic strontium- titanate", *Phys. Rev.* 123, 97 (1961).

- [16] V. L. Gurevich and A. K. Tagantsev, "Intrinsic dielectric loss in crystals", *Adv. Phys.* 40, 719 (1991).
- [17] A. K. Tagantsev, "Phonon mechanisms of intrinsic dielectric loss in crystals", in "Ferroelectric Ceramics", N. Setter and E. L. Colla, eds. (Birkhäuser, Basel), 127 (1993).
- [18] T. Mitsui and S. Nomura, in "LANDOLT-BÖRNSTEIN numerical data and functional relationships in science and technology", K. -H. Hellwege and A. M. Hellwege, eds. (Springer-Verlag, Berlin), vol. 16 (a) (1981).
- [19] E. Nakamura, in "LANDOLT-BÖRNSTEIN numerical data and functional relationships in science and technology", T. Mitsui and E. Nakamura, eds. (Springer-Verlag, Berlin), vol. 28 (1990).
- [20] D. Kirillov, Y. Suzuki, L. Antognazza, K. Char, I. Bozovic, and T. H. Geballe, "Phonon anomalies at the magnetic phase transition in SrRuO<sub>3</sub>", *Phys. Rev. B* 51, 12825 (1995).
- [21] Vladimir I. Merkulov, Jon R. Fox, Hong-Cheng Li, Weidong Si, A. A. Sirenko, and X. X. Xi, "Metal-oxide bilayer raman scattering in SrTiO<sub>3</sub> thin films", *Appl. Phys. Lett.* 72, 3291 (1998).
- [22] W. G. Nilsen and J. G. Skinner, "Raman spectrum of strontium titanate", *J. Chem. Phys.* 48, 2240 (1968).
- [23] V. N. Denisov, B. N. Mavrin, and V. B. Podobedov, "Hyper-Raman scattering by vibrational excitations in crystals, glasses and liquids", *Phys. Rep.* 151, 1 (1987).
- [24] H. Vogt and G. Rossbroich, "Accurate determination of the far-infrared dispersion in SrTiO<sub>3</sub> by hyper-Raman spectroscopy", *Phys. Rev. B* 24, 3086 (1981).
- [25] U. Fano, "Effects of configuration interaction on intensities and phase shifts", *Phys. Rev.* 124, 1866 (1961).
- [26] S. K. Manlief and H. Y. Fan, "Raman spectrum of KTa<sub>0.64</sub>Nb<sub>0.36</sub>O<sub>3</sub>", *Phys. Rev. B* 5, 4046 (1972).
- [27] U. Bianchi, W. Kleemann, and J. G. Bednorz, "Raman scattering of ferroelectric Sr<sub>1-x</sub>Ca<sub>x</sub>TiO<sub>3</sub>, x = 0.007", *J. Phys.: Condens. Matter* 6, 1229 (1994).
- [28] J. Toulouse, P. DiAntonio, B. E. Vugmeister, X. M. Wang, and L. A. Knaus, "Precursor effects and ferroelectric microregions in KTa<sub>1-x</sub>Nb<sub>x</sub>O<sub>3</sub> and K<sub>1-y</sub>Li<sub>y</sub>TaO<sub>3</sub>", *Phys. Rev. Lett.* 68, 232 (1992).
- [29] R. Waser and D. M. Smyth, "Defect chemistry, conduction, and breakdown mechanism of perovskite-structure titanates", in "Ferroelectric thin films: synthesis and basic properties", Carlos Paz de Araujo, James F. Scott, and George W. Taylor, eds. (Gordon and Breach Publishers, Amsterdam), 47 (1996).
- [30] H. Uwe, H. Yamaguchi, and T. Sakodo, "Ferroelectric microregion in KT<sub>1-x</sub>Nb<sub>x</sub>O<sub>3</sub> and SrTiO<sub>3</sub>", *Ferroelectrics* 96, 123 (1989).

- [31] S. A. Prosandeyev, A. V. Fisenko, A. I. Riabchinski, I. A. Osipenko, I. P. Raevski, and N. Safontseva, "Study of intrinsic point defects in oxides of the perovskite family: I. Theory", *J. Phys.: Condens. Matter* 8, 6705 (1996).
- [32] I. P. Raevski, S. M. Maksimov, A. V. Fisenko, S. A. Prosandeyev, I. A. Osipenko, and P. F. Tarasenko, "Study of intrinsic point defects in oxides of the perovskite family: II. Experiment", *J. Phys.: Condens. Matter* 10, 8015 (1998).
- [33] A. A. Sirenko, I. A. Akimov, J. R. Fox, A. M. Clark, Hong-Cheng Li, Weidong Si, and X. X. Xi, "Observation of the first-order raman scattering in SrTiO<sub>3</sub> thin films", *Phys. Rev. Lett.* 82, 4500 (1999).
- [34] D. W. Berreman, "Infrared absorption at longitudinal optic frequency in cubic crystal films", *Phys. Rev.* 130, 2193 (1963).
- [35] H. Vogt, "Refined treatment of the model of linearly coupled anharmonic oscillators and its application to the temperature dependence of the zone-center soft-mode frequencies of KTaO<sub>3</sub> and SrTiO<sub>3</sub>", *Phys. Rev. B* 51, 8046 (1995).
- [36] I. Fedorov, V. Zelezny, J. Petzelt, V. Trepakov, M. Jelinek, V. Trtik, M. Cernansky, and V. Studnicka, "Far-infrared spectroscopy of a SrTiO<sub>3</sub> thin film", *Ferroelectrics* 208, 413 (1998).
- [37] C. Zhou and D. M. Newns, "Intrinsic dead layer effect and the performance of ferroelectric thin film capacitors", *J. Appl. Phys.* 82, 3081 (1997).
- [38] C. Basceri, S. K. Streiffer, A. I. Kingon, and R. Waser, "The dielectric response as a function of temperature and film thickness of fiber-textured (Ba, Sr)TiO<sub>3</sub> thin films grown by chemical vapor deposition", *J. Appl. Phys.* 82, 2497 (1997).
- [39] C. T. Black and J. J. Welser, "Electric-field penetration into metals: Consequences for high-dielectric-constant capacitors", *IEEE Trans. Electron Devices* 46, 776 (1999).
- [40] H. -C. Li, Weidong Si, Alexander D. West, and X. X. Xi, "Thickness dependence of dielectric loss in SrTiO<sub>3</sub> thin films", *Appl. Phys. Lett.* 73, 464 (1998).
- [41] A. A. Sirenko, C. Bernhard, A. Golnik, A. M. Clark, Jianhua Hao, Weidong Si, and X. X. Xi, "Soft-mode hardening in SrTiO<sub>3</sub> thin films", *Nature* 404, 373 (2000).
- [42] J. Hemberger, P. Lunkenheimer, R. Viana, R. Böhmer, and A. Loidl, "Electric-field-dependent dielectric constant and nonlinear susceptibility in SrTiO<sub>3</sub>", *Phys. Rev. B* 52, 13159 (1995).
- [43] H. -C. Li, Weidong Si, Alexander D. West, and X. X. Xi, "Near single crystal-level dielectric loss and nonlinearity in pulsed laser deposited SrTiO<sub>3</sub> thin films", *Appl. Phys. Lett.* 73, 190 (1998).
- [44] P. A. Fleury and J. M. Worlock, "Electric-field-induced Raman scattering in SrTiO<sub>3</sub> and KTaO<sub>3</sub>", *Phys. Rev.* 174, 613 (1968).
- [45] B. O. Wells, M. V. Zimmerman, S. M. Shapiro, Y. Zhu, H. Nakao, A. M. Clark, and X. X. Xi, "Anomalous structural phase transitions in SrTiO<sub>3</sub> thin films", unpublished.

- [46] I. A. Akimov, A. A. Sirenko, A. M. Clark, Jianhua Hao, and X. X. Xi, "Electric-field induced soft-mode hardening in SrTiO<sub>3</sub> films", *Phys. Rev. Lett.* 84, 4625 (2000).